INAUGURAL ARTICLE

PLANT BIOLOGY

Identification of SLAC1 anion channel residues required for CO_2/bicarbonate sensing and regulation of stomatal movements

Jingbo Zhang[a], Nuo Wang[b], Yinglong Miao[b,c,d,1], Felix Hauser[a], J. Andrew McCammon[b], Wouter-Jan Rappel[e], and Julian I. Schroeder[a,1]

[a]Cell and Developmental Biology Section, Division of Biological Sciences, University of California, San Diego, La Jolla, CA 92093-0116; [b]Department of Chemistry and Biochemistry, University of California, San Diego, La Jolla, CA 92093; [c]Center for Computational Biology, University of Kansas, Lawrence, KS 66047; [d]Department of Molecular Biosciences, University of Kansas, Lawrence, KS 66045; and [e]Department of Physics, University of California, San Diego, La Jolla, CA 92093-0354

This contribution is part of the special series of Inaugural Articles by members of the National Academy of Sciences elected in 2015.

Contributed by Julian I. Schroeder, September 5, 2018 (sent for review May 2, 2018; reviewed by Donald Hamelberg and Yi-Fang Tsay)

Increases in CO_2 concentration in plant leaves due to respiration in the dark and the continuing atmospheric [CO_2] rise cause closing of stomatal pores, thus affecting plant–water relations globally. However, the underlying CO_2/bicarbonate (CO_2/HCO_3^-) sensing mechanisms remain unknown. [CO_2] elevation in leaves triggers stomatal closure by anion efflux mediated via the SLAC1 anion channel localized in the plasma membrane of guard cells. Previous reconstitution analysis has suggested that intracellular bicarbonate ions might directly up-regulate SLAC1 channel activity. However, whether such a CO_2/HCO_3^- regulation of SLAC1 is relevant for CO_2 control of stomatal movements in planta remains unknown. Here, we computationally probe for candidate bicarbonate-interacting sites within the SLAC1 anion channel via long-timescale Gaussian accelerated molecular dynamics (GaMD) simulations. Mutations of two putative bicarbonate-interacting residues, R256 and R321, impaired the enhancement of the SLAC1 anion channel activity by CO_2/HCO_3^- in *Xenopus* oocytes. Mutations of the neighboring charged amino acid K255 and residue R432 and the predicted gate residue F450 did not affect HCO_3^- regulation of SLAC1. Notably, gas-exchange experiments with *slac1*-transformed plants expressing mutated SLAC1 proteins revealed that the SLAC1 residue R256 is required for CO_2 regulation of stomatal movements in planta, but not for abscisic acid (ABA)-induced stomatal closing. Patch clamp analyses of guard cells show that activation of S-type anion channels by CO_2/HCO_3^-, but not by ABA, was impaired, indicating the relevance of R256 for CO_2 signal transduction. Together, these analyses suggest that the SLAC1 anion channel is one of the physiologically relevant CO_2/HCO_3^- sensors in guard cells.

SLAC1 | CO_2 signal | GaMD simulation | stomatal movement | carbon dioxide

On the surface of leaves of land plants, pairs of specialized epidermal cells, the guard cells, form stomatal pores. These pores regulate gas exchange between the intercellular spaces of leaves and the atmosphere to optimally balance CO_2 uptake for photosynthesis and water loss. Stomatal apertures are regulated by several environmental factors, including light, drought, CO_2 concentration, relative humidity, and pathogens (1–5). In darkness, respiration in leaves causes an increase in the CO_2 concentration in the intercellular spaces inside leaves (6), and this increase causes closing of stomatal pores (7). Furthermore, the continuing rise in the CO_2 concentration in the atmosphere causes reduced stomatal apertures globally, increases plant leaf temperatures, and is predicted to affect yields (1, 8, 9). However, compared with the relatively well-studied abscisic acid (ABA)-mediated stomatal closure mechanisms (3), the mechanisms by which CO_2 controls stomatal movements remain to a large degree unclear and fragmented.

Stomatal closure is triggered by the release of anions from plant guard cells via S-type anion channels (10, 11), encoded by the *SLAC1* (SLOW ANION CHANNEL-ASSOCIATED 1) gene (12, 13). The OST1 (OPEN STOMATA 1) protein kinase is required for CO_2-induced stomatal closing (14). In contrast, the HT1 (HIGH LEAF TEMPERATURE 1) protein kinase negatively regulates high CO_2-induced stomatal closing (15). SLAC1 is activated in *Xenopus* oocytes by a group of protein kinases, including OST1, Ca^{2+}-dependent protein kinases, and the GHR1 (GUARD CELL HYDROGEN PEROXIDE-RESISTANT 1) membrane protein (16–21). Furthermore, the mitogen-activated protein kinase MPK12 and RHC1 (RESISTANT TO HIGH CO_2), a MATE-type anion transporter, have been reported to regulate stomatal closure in response to high CO_2 (21–23). Recently, two protein kinases, CBC1 and CBC2 (CONVERGENCE OF BLUE LIGHT AND CO_2), were shown to be phosphorylated by both HT1 and the blue light receptor phot1 (24). *cbc1cbc2* double-mutant plants displayed an interruption of stomatal opening in response to blue light and

Significance

Plants optimize CO_2 influx for photosynthesis and water loss by regulating gas exchange between the inside of leaves and the atmosphere via stomatal pores. Respiration in darkness and the continuing atmospheric [CO_2] rise cause closing of stomatal pores, thus affecting plant water loss globally. However, the mechanisms by which plant guard and mesophyll cells sense CO_2/bicarbonate for CO_2 regulation of stomata remain unknown. Here, a computer-aided modeling approach and multiple experimental assays suggest that the anion channel SLAC1 plays an important role in CO_2/bicarbonate sensing in guard cells. This work will aid in the understanding of how plants cope with the increasing CO_2 concentration and can further lead to new approaches for developing crop plants to adapt to climate change.

Author contributions: J.Z., J.A.M., W.-J.R., and J.I.S. designed research; J.Z., N.W., Y.M., F.H., and W.-J.R. performed research; J.Z., N.W., and Y.M. analyzed data; and J.Z., Y.M., and J.I.S. wrote the paper.

Reviewers: D.H., Georgia State University; and Y.-F.T., Academia Sinica.

The authors declare no conflict of interest.

See Profile on page 11109.

[1]To whom correspondence may be addressed. Email: jischroeder@ucsd.edu or miao@ku.edu.

This article contains supporting information online at www.pnas.org/lookup/suppl/doi:10.1073/pnas.1807624115/-/DCSupplemental.

Published online October 9, 2018.

low CO_2, revealing a convergent site of blue light and CO_2 signaling in guard cells (24).

In guard cells, carbonic anhydrases accelerate the catalysis of CO_2 molecules to bicarbonate and protons. Disruption of two carbonic anhydrase genes, *βCA1* and *βCA4*, causes an impairment in the stomatal CO_2 response in *Arabidopsis* (25). Similarly, disruption of the rice carbonic anhydrase gene *OsβCA1* and the maize *ZmCA1* and *ZmCA2* genes impair CO_2 control of stomatal movements (26, 27). These carbonic anhydrases function as catalytic enzymes rather than as conventional CO_2 receptors/sensors (25). While several components in the CO_2 signaling pathway have been identified, the mechanisms by which plants sense the CO_2 signal to regulate stomatal movements remain enigmatic. Studies have suggested that intracellular HCO_3^- ions activate S-type anion channels in the guard cell plasma membrane (14, 22, 24, 25, 28). Direct injection of bicarbonate enables an enhancement of SLAC1-mediated currents in *Xenopus* oocytes independent of the coexpressed protein kinase (29), further suggesting that intracellular bicarbonate may directly up-regulate SLAC1 channel activity. However, the mechanism by which CO_2/bicarbonate (CO_2/HCO_3^-) enhances SLAC1 anion channel activity and the sites of SLAC1 that may perceive CO_2 signals are unknown. Moreover, any relevance of the intracellular CO_2/HCO_3^- enhancement of SLAC1 activity in oocytes for CO_2 control of stomatal movements in planta remains completely unknown.

Gaussian accelerated molecular dynamics (GaMD) provides both unconstrained enhanced sampling and accurate energetic reweighting for free energy calculations of large proteins (30). GaMD, a variation of the aMD method (31), applies a harmonic boost potential to smooth the biomolecular potential energy surface and reduce energy barriers in proteins. GaMD accelerates the modeling of protein conformational transitions and ligand binding by orders of magnitude (30). Thus, GaMD enables the characterization of complex biomolecular conformational changes in large proteins quantitatively (32). GaMD is particularly advantageous for studying "free" small-molecule interaction processes with large proteins (30) and serves as a promising tool for biomolecular conformation sampling of small-molecule interactions, prediction of drug–receptor interactions, and computer-aided drug design and discovery (33, 34). GaMD simulations have not yet been applied to plant proteins.

In this study, we applied GaMD to computationally seek putative bicarbonate-interacting sites in the SLAC1 channel. By using several independent experimental assays, the most probable candidate intracellular bicarbonate-interacting sites in SLAC1 were investigated in vitro and in planta. Residue R256 was uncovered to be required for CO_2 regulation of SLAC1 activity and CO_2 control of stomatal movements, but not for ABA responses in guard cells. Together, the present findings support the model that SLAC1 is one of the bicarbonate sensors in guard cells, functioning in CO_2 control of stomatal movements.

Results

GaMD Simulations of Bicarbonate Ion Interactions with SLAC1. Previous studies showed that cytoplasmic CO_2/HCO_3^- up-regulates SLAC1 activity in *Xenopus* oocytes (29). To further investigate possible mechanisms underlying CO_2/HCO_3^- regulation of SLAC1 channel activity, we conducted GaMD simulations of bicarbonate binding to the SLAC1 anion channel. The simulations allowed us to determine energetically preferred binding sites of bicarbonate ions in the SLAC1 protein. Based on the template structure of the SLAC1 homolog TehA, which shares 19% sequence identity with the SLAC1 transmembrane region (35), the structure of SLAC1 was modeled using three independent modeling algorithms (ModBase, iTasser, and RaptorX) (36–38). These algorithms generated overall-similar channel structures of SLAC1. By using the MatchMaker function provided in UCSF Chimera v1.12 (https://www.cgl.ucsf.edu/chimera/), the ModBase algorithm produced a better fit compared with iTasser and RaptorX. The predicted structure generated by ModBase is shown in Fig. 1*A*. Next, the CHARMM-Graphic User Interface (GUI) (www.charmm-gui.org) (39) was applied to embed SLAC1 in a palmitoyl-oleoyl phosphatidylcholine (POPC) lipid bilayer. Water and ions were added to generate the final membrane-protein system for dynamic simulations (Fig. 1*B*).

Previous findings showed that intracellular HCO_3^-, but not extracellular HCO_3^-, activates SLAC1 anion channels (14, 22, 24, 29). This guided us to focus on sites exposed to the cytosolic solution phase. For the simulations, initial energy minimization and thermalization of the SLAC1 system followed the same protocol as used in previous studies of membrane proteins (32, 40). GaMD simulations were then performed using the dual-boost scheme with the threshold energy E set to V_{max} (*SI Appendix, Supplemental Methods*). The simulations included 2-ns conventional MD, 50-ns equilibration after adding the boost potential, and then three independent 100-ns production runs with randomized initial atomic velocities. Analysis of GaMD simulations suggested that residues K255, R256, and R321 of SLAC1 had high probabilities of interactions with bicarbonate ions in the following order: R321 > R256 > K255 (Fig. 1*C*). Even though residue R432 was predicted not to represent a bicarbonate-interacting site (Fig. 1*C*), we included R432 as a control residue, as R432 is a fully conserved positively charged residue in the SLAC1/SLAH family in *Arabidopsis* and it is predicted to face the intracellular space (Fig. 1 *A* and *D*). SLAC1 residues K255, R256, R321, and R432, as well as the proposed gate residue inside the SLAC1 channel pore, F450 (35), were selected for further mutagenesis and experimental analyses (Fig. 1 *C* and *D*).

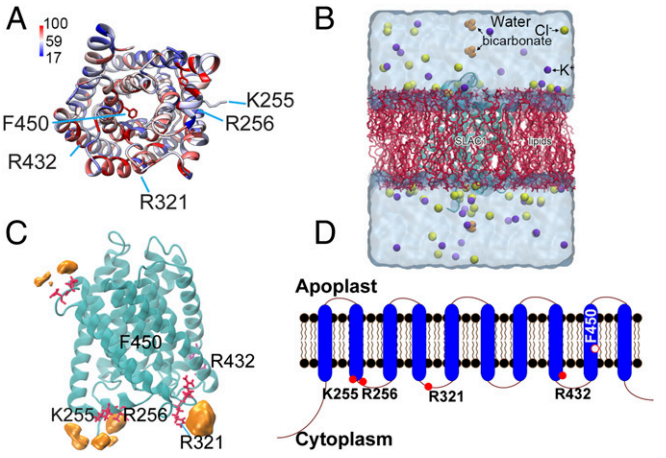

Fig. 1. Computationally predicted SLAC1 protein structure and its potential bicarbonate binding sites. (*A*) Predicted structure of SLAC1 transmembrane domains. The structure was predicted as described using modeling algorithms and coordinates of the TehA template structure (35) and is pseudo-colored based on sequence conservation among *Arabidopsis* SLAC/SLAH homologs and TehA. Blue and red respectively correspond to 17% and 100% conservation with AtSLAC1/SLAH homologous and TehA. (*B*) The simulation system is shown. The SLAC1 structure was embedded in a POPC lipid membrane using the CHARMM-GUI Membrane Builder. Bicarbonate was added to the model afterward (see *Materials and Methods*). The final simulation system of SLAC1 had dimensions of 83 × 83 × 105 Å^3, with a total of ~65,000 atoms. (*C*) Key residues (red) and probability of bicarbonate interaction map (orange). F450 is the proposed gate residue of SLAC1; K255, R256, and R321 are residues predicted to interact with bicarbonate during GaMD simulations; and R432 is the conserved control residue for which bicarbonate is predicted not to bind in simulations. (*D*) The SLAC1 protein is predicted to form 10 transmembrane α-helices with the N and C termini located in the cytoplasm. Filled red circles indicate the location of amino acids shown in *A* and *C*; the open red circle indicates the proposed channel gate residue.

Substitution of R256 or R321 by Alanine Impairs Bicarbonate Enhancement of SLAC1 Channel Activity in *Xenopus* Oocytes. To analyze the role of these four residues (K255, R256, R321, and R432), we first substituted them with alanine by site-directed mutagenesis and monitored whether these mutations affect SLAC1 channel functionality. We coexpressed the SLAC1 mutant channels with the OST1 protein kinase in *Xenopus* oocytes and, subsequently, analyzed the functionality of SLAC1 isoforms by performing two-electrode voltage clamp analyses as previously described (16, 17, 29). Although K255 and R256 are partially conserved and R321 is fully conserved in the *Arabidopsis* SLAC1/SLAH gene family, individual substitution of K255, R256, or R321 by alanine had no impact on the average magnitude of SLAC1-mediated currents, which were similar to wild-type (WT) SLAC1 (Fig. 2; 3 oocyte batches, 9 to 14 oocytes per condition in each batch; *SI Appendix*, Fig. S1). However, alanine replacement of R432, which is a fully conserved positively charged residue in the SLAC1/SLAH gene family in *Arabidopsis* (Fig. 1*A*), caused only background-like currents in *Xenopus* oocytes (*SI Appendix*, Fig. S1), suggesting that R432 is a key residue for maintaining SLAC1 channel function.

Residue F450 was reported to act as a gate residue inside the SLAC1 pore (35). Consistent with this previous report, coexpression of OST1 with a SLAC1-F450A mutant caused a more linear current–voltage relationship compared with WT SLAC1 in the same batch of *Xenopus* oocytes (*SI Appendix*, Fig. S2). However, expression of SLAC1-F450A alone without a protein kinase in *Xenopus* oocytes generated very small background currents similar to WT SLAC1 without a coexpressed kinase (*SI Appendix*, Fig. S2; 3 independent oocyte batches).

SLAC1 currents have been shown to be enhanced by cytoplasmic bicarbonate anions (HCO_3^-) in *Xenopus* oocytes, and sodium bicarbonate ($NaHCO_3$) injection into control H_2O-injected oocytes has been shown not to affect background current activities of oocytes (29). To further investigate whether the above functional SLAC1 mutations (K255A, R256A, R321A, and F450A) have an effect on HCO_3^- activation of SLAC1, we injected $NaHCO_3$ into oocytes individually expressing these SLAC1 isoforms with OST1. Two-electrode voltage clamp analyses revealed that SLAC1-R256A and SLAC1-R321A impaired bicarbonate enhancement of SLAC1-mediated currents in *Xenopus* oocytes (Figs. 2 and 3). Furthermore, expression of the SLAC1 double-mutant isoform SLAC1-R256A-R321A in *Xenopus* oocytes showed impairment of bicarbonate activation of SLAC1 currents (*SI Appendix*, Fig. S3; 3 oocyte batches). Enhancement of WT SLAC1 currents by bicarbonate was

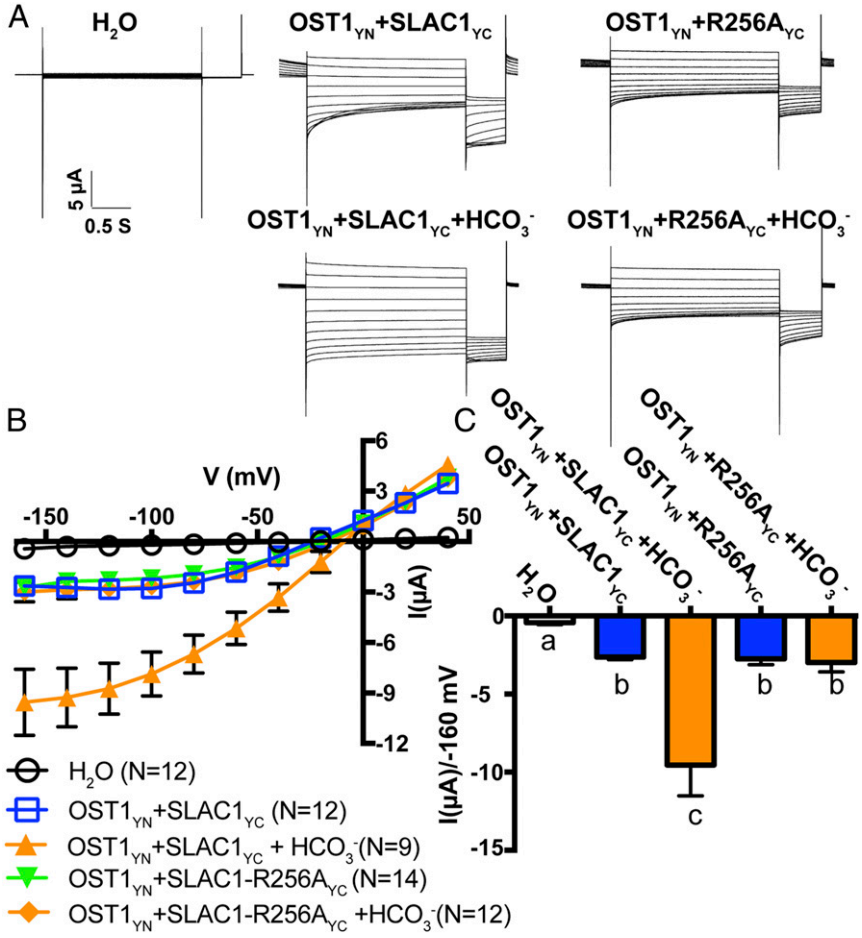

Fig. 2. Impact of R256 mutation on bicarbonate enhancement of SLAC1-mediated currents. (*A*) Representative whole-cell Cl^- current recordings in oocytes coexpressing SLAC1yc or SLAC1-R256Ayc with OST1yn. Currents were recorded in response to 3-s voltage pulses ranging from +40 mV to −160 mV in −20 mV steps, with a holding potential at 0 mV followed by −120 mV after voltage pulses. (*B*) Mean current–voltage curves of oocytes coexpressing the indicated proteins with or without $NaHCO_3$ injection. (*C*) Average currents of the indicated SLAC1 isoforms with and without injection of 11.5 mM bicarbonate (14, 22, 29) at −160 mV. The bath solution contained 10 mM MES/Tris (pH = 7.4), 1 mM $MgCl_2$, 1 mM $CaCl_2$, 2 mM HCl, 24 mM NaCl, and 70 mM sodium gluconate. Three independent batches of oocytes showed similar results (n = 9 to 14 oocytes from each oocyte batch per condition). Error bars denote mean ± SEM. Means with letters (a, b, and c) are grouped based on one-way ANOVA and Tukey's test, $P < 0.05$.

consistently observed in positive-control experiments in all batches of oocytes (e.g., Figs. 2 and 3 and *SI Appendix*, Fig. S3). Bicarbonate enhancement of SLAC1-mediated currents remained intact in oocytes expressing SLAC1-K255A and SLAC1-F450A (*SI Appendix*, Fig. S4; 3 oocyte batches). Our results indicate that the SLAC1 residues R256 and R321 are required for intracellular bicarbonate enhancement of SLAC1-mediated currents in *Xenopus* oocytes.

Mutation of R256 Affects Stomatal Movement Response to CO_2 in Planta. Plants rapidly close or open stomata in response to CO_2 concentration shifts, and SLAC1 is a key mediator of stomatal movements (12, 13). To investigate whether mutation of R256A or R321A on SLAC1 affects the stomatal CO_2 response in vivo, we generated transgenic plants by transforming two *slac1* mutant alleles, *slac1-1* and *slac1-3*, with a construct harboring the genomic *SLAC1* sequence fused to its native promoter. SLAC1 protein was fused at the SLAC1 C terminus to the fluorescent protein mVENUS (41) to monitor the expression of SLAC1 protein in guard cells of transgenic plants (Fig. 4*A*). Gas-exchange analyses of intact leaves of transgenic *slac1-1* plants showed that the expression of SLAC1-R256A was not able to fully restore CO_2-regulated stomatal movements (Fig. 4 *B* and *C*). Two independent lines, *slac1-1*/SLAC1pro::R256A#5::mVENUS and *slac1-1*/SLAC1pro::R256A#7::mVENUS, displayed slower CO_2 responses compared with control plants expressing the WT SLAC1 in the *slac1-1* background (Fig. 4 *B* and *C*). Analysis of fits of one-phase exponential functions to the data showed that the response kinetics of stomatal closing to CO_2 elevation were significantly slower in the SLAC1-R256A#5 (τ = 12.88 ± 1.53 min) and SLAC1-R256A#7 (τ = 12.20 ± 1.92 min) lines compared with the SLAC1-WT line (τ = 4.48 ± 0.42 min) (R256A#5 vs. SLAC1-WT, $P < 0.05$; R256A#7 vs. SLAC1-WT, $P < 0.05$; one-way ANOVA and Tukey's test). We also examined the intensity of mVENUS fluorescence in guard cells of these transgenic lines. SLAC1-WT and SLAC1-R256A lines had similar average mVENUS fluorescence intensities (*SI Appendix*, Fig. S5), suggesting that the CO_2 response impairment in SLAC1-R256A transgenic lines was not due to varied protein expression levels of the SLAC1 protein. Similar stomatal closing responses to CO_2 elevation were observed in two independent *slac1-3* transgenic lines, confirming that the SLAC1-R256A mutation reduces the stomatal CO_2 response in planta (Fig. 4 *D* and *E*).

In contrast to SLAC1-R256A–expressing lines, transgenic lines expressing SLAC1-R321A (Fig. 5*A*) showed similar stomatal CO_2 responses as SLAC1-WT–expressing plants, suggesting that in its biological protein environment, this site does not affect the physiological CO_2 response. Furthermore, transgenic lines expressing SLAC1-K255A in the *slac1-1* background showed similar stomatal CO_2 responses as WT plants (Fig. 5*B*). Transgenic plants expressing the nonfunctional SLAC1-R432A isoform in the *slac1-1* background displayed an interrupted stomatal response to high CO_2 but, interestingly, also displayed an intact response to low CO_2, implicating low CO_2 regulation of proton pumps and other channels/transporters (Fig. 5*C*).

Steady-state stomatal conductance values were lower when functional SLAC1 isoforms were independently expressed in *slac1* mutant alleles (Figs. 4 and 5). Because transgenic lines expressing

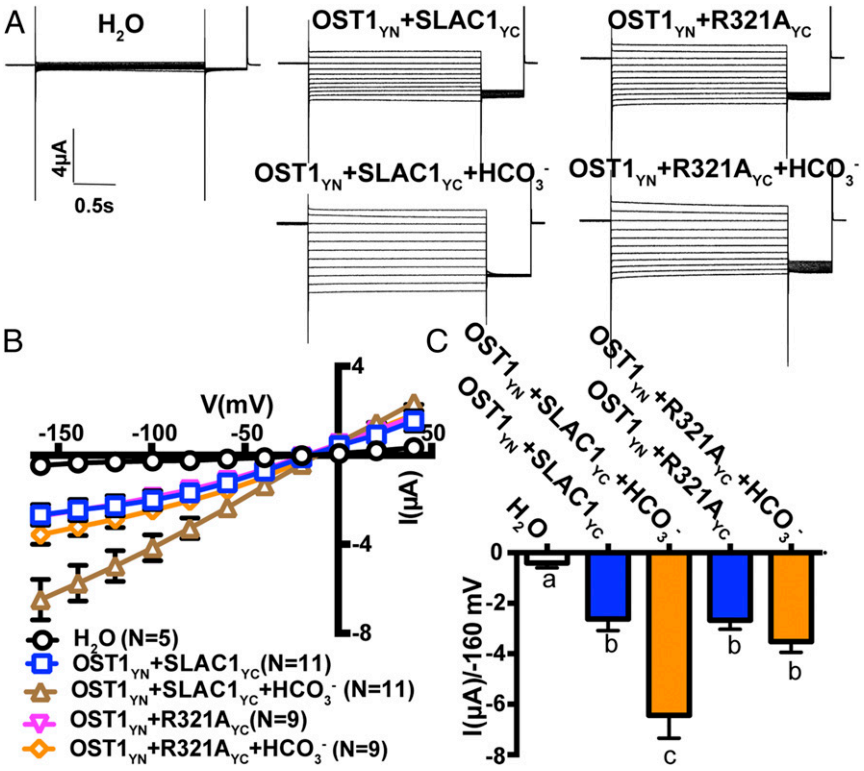

Fig. 3. Impact of R321 mutation on bicarbonate enhancement of SLAC1. (*A*) Representative whole-cell Cl^- current recordings in oocytes coexpressing SLAC1yc or SLAC1-R321Ayc with OST1yn. Currents were recorded in response to 3-s voltage pulses ranging from +40 mV to −160 mV in −20 mV steps, with a holding potential of 0 mV and return to −120 mV after voltage pulses. The bath solution contained 10 mM MES/Tris (pH = 7.4), 1 mM $MgCl_2$, 1 mM $CaCl_2$, 2 mM HCl, 24 mM NaCl, and 70 mM sodium gluconate. (*B*) Mean current–voltage curves of oocytes coexpressing the indicated proteins and the indicated HCO_3^- injection. (*C*) Average currents of the indicated SLAC1 isoforms with and without injection of bicarbonate at −160 mV. Error bars denote mean ± SEM. Means with different letters are grouped based on one-way ANOVA and Tukey's test, $P < 0.05$. Three independent batches of oocytes showed similar results (n = 5 to 11 oocytes from each oocyte batch per condition).

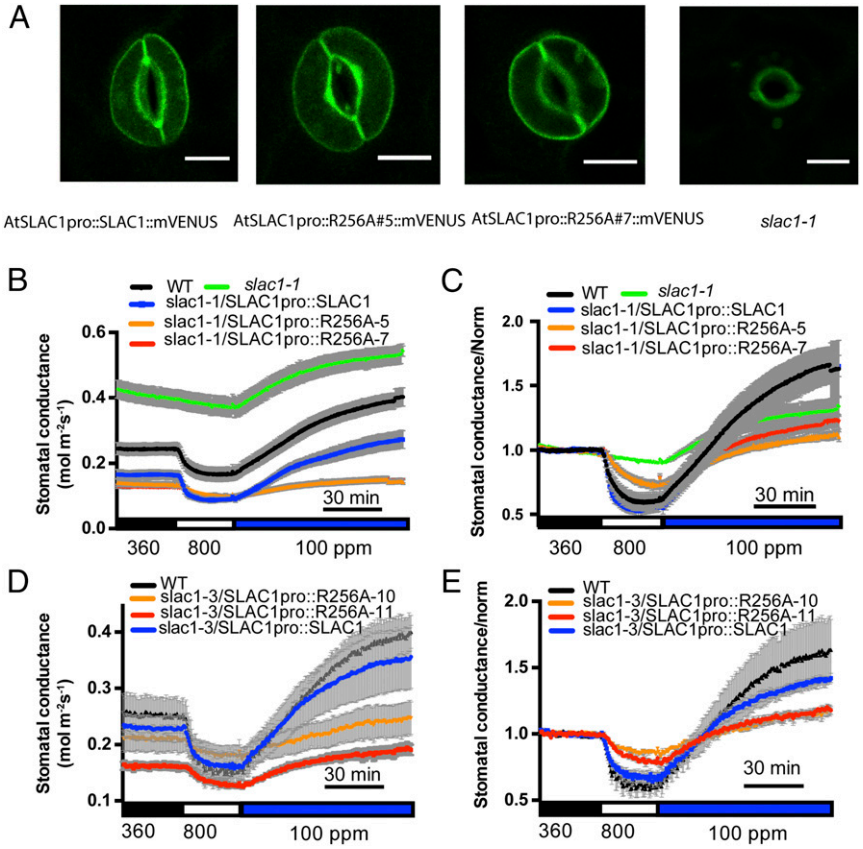

Fig. 4. Expression of SLAC1-R256A in *slac1* mutant alleles impairs CO_2-regulated stomatal conductance. (*A*) *slac1-1* guard cells are shown expressing the indicated SLAC1-mVENUS fusion isoforms. All images were taken under the same confocal microscopy intensity parameters. (Scale bar: 10 μm.) (*B* and *D*) Stomatal conductance of WT and *slac1* plants transformed with SLAC1pro::SLAC1 and SLAC1pro::SLAC1-R256A in the *slac1-1* background (*B*) and the *slac1-3* background (*D*) in response to ambient CO_2 changes. For *B*: WT, $n = 5$; SLAC1pro::SLAC1::mVENUS, $n = 5$; SLAC1pro::R256A#5::mVENUS, $n = 8$; SLAC1pro::R256A#7::mVENUS, $n = 9$; and *slac1-1*, $n = 3$. For *D*: WT, $n = 3$; SLAC1pro::SLAC1::mVENUS, $n = 5$; SLAC1pro::R256A#10::mVENUS, $n = 3$; and SLAC1pro::R256A#11::mVENUS, $n = 3$). Note that in *B*, SLAC1pro::R256A#7::mVENUS data points are not clearly visible, as they overlap with data from SLAC1pro::R256A#5::mVENUS. (*C* and *E*) Normalized data shown in *B* and *D*, respectively. Data were normalized relative to average stomatal conductance during 30 min of 360-ppm CO_2 exposure before CO_2 elevation. Error bars denote mean ± SEM.

SLAC1-R256A had a lower steady-state stomatal conductance (Fig. 4 *B* and *D*), we investigated the stomatal index and density of transgenic and WT plants. No significant difference was observed (*SI Appendix*, Fig. S6; stomatal index: R256A#5 vs. SLAC1-WT, $P = 0.91$; R256A#7 vs. SLAC1-WT, $P = 0.87$; stomatal density: R256A#5 vs. SLAC1-WT, $P = 0.10$; R256A#7 vs. SLAC1-WT, $P = 0.33$; one-way ANOVA and Tukey's test), suggesting that expression of SLAC1-R256A did not affect stomatal development.

ABA induces stomatal closure. To investigate whether expression of SLAC1-R256A has an effect on ABA-induced stomatal closing in planta, we carried out gas-exchange experiments with ABA application to the transpiration stream via the petiole of leaves. Two independent transgenic lines expressing SLAC1-R256A in the *slac1-1* background—*slac1-1*/SLAC1pro::R256A#5::mVENUS and *slac1-1*/SLAC1pro::R256A#7::mVENUS—showed similar ABA-induced stomatal closing kinetics and magnitudes compared with leaves expressing SLAC1-WT in *slac1-1* (Fig. 6), indicating that the SLAC1-R256A mutation affects the stomatal CO_2 response, but not the ABA response in planta.

CO_2/HCO_3^--Activated S-Type Anion Channel Currents Are Impaired in SLAC1-R256A Transgenic Plants. Elevated concentrations of cytoplasmic HCO_3^- have been shown to activate S-type anion channel currents in the plasma membrane of guard cells (14, 22–25, 28). To investigate whether the above-described impairment in the stomatal CO_2 response of SLAC1-R256A–expressing transgenic lines is linked to S-type anion current regulation in guard cells, we isolated guard cell protoplasts from 4- to 6-wk-old plants of WT and transgenic lines expressing SLAC1-WT and SLAC1-R256A in the *slac1-1* background. Whole-cell patch clamp experiments were carried out with addition of $CsHCO_3$ to the patch clamp pipette solution that dialyzes the cytosol. These experiments showed that the HCO_3^- activation of S-type anion channel currents was significantly impaired in guard cells of two independent transgenic lines expressing SLAC1-R256A (Fig. 7; at −145 mV: SLAC1-R256A#5 vs. SLAC1-WT, $P < 0.001$; SLAC1-R256A#7 vs. SLAC1-WT, $P < 0.001$; one-way ANOVA with Tukey's test). However, the HCO_3^--activated S-type anion channel currents in transgenic lines expressing SLAC1-WT had a similar magnitude as WT plants (Fig. 7; at −145 mV: SLAC1-R256A#5 vs. SLAC1-WT, $P = 0.98$; SLAC1-R256A#7 vs. SLAC1-WT, $P = 0.06$; one-way ANOVA with Tukey's test).

When isolated guard cell protoplasts were exposed to ABA, ABA activation of S-type anion channel currents in guard cells of SLAC1-R256A–expressing transgenic lines was comparable with ABA activation in WT and SLAC1-WT–expressing guard cells (Fig. 8). These electrophysiological results are consistent with the above-described stomatal conductance analyses in intact leaves in response to CO_2 and ABA (Figs. 4 and 6), further supporting the model that the SLAC1 residue R256 is important for CO_2-induced stomatal closing and stomatal CO_2 signal transduction in planta, but not for ABA responses.

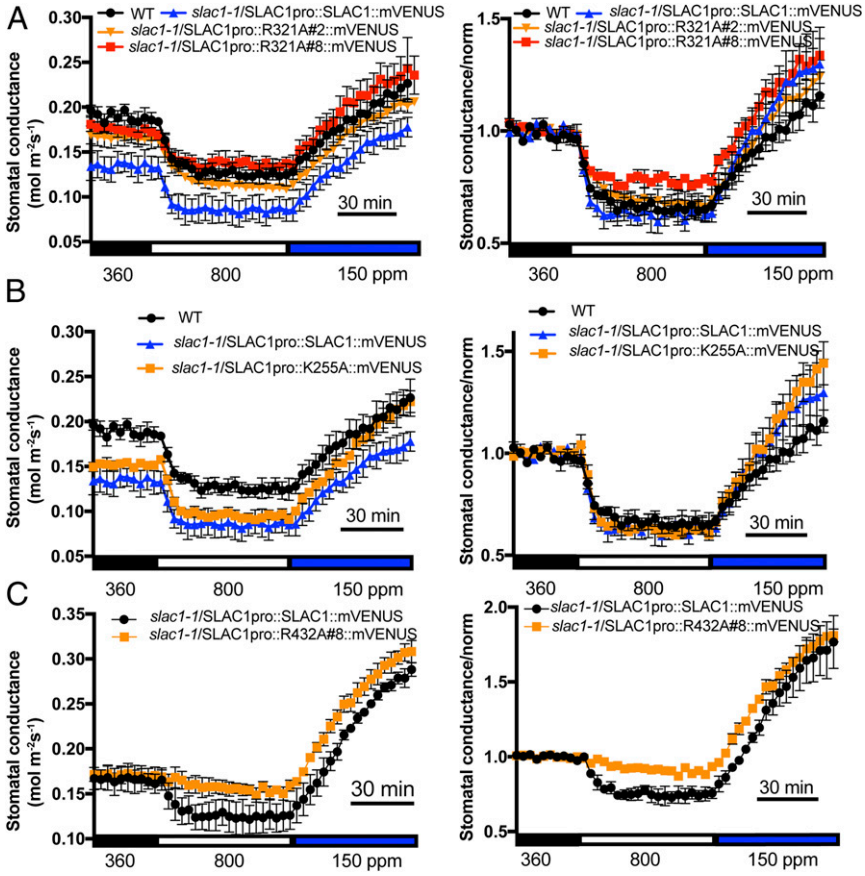

Fig. 5. Effect of point mutations R321, K255, and R432 in SLAC1 on CO_2 response in *slac1*-transformed lines. Stomatal conductance of WT and *slac1* transgenic plants expressing the indicated SLAC1 isoforms in the *slac1-1* background in response to ambient CO_2 changes. (*A*) SLAC1-R321A (WT, $n = 3$; SLAC1pro::SLAC1::mVENUS, $n = 3$; SLAC1pro::R321A#2::mVENUS, $n = 4$; and SLAC1pro::R321A#8::mVENUS, $n = 3$). (*B*) SLAC1-K255A (WT, $n = 3$; SLAC1pro::SLAC1::mVENUS, $n = 3$; and SLAC1pro::K255A::mVENUS, $n = 3$). (*C*) SLAC1-R432A (SLAC1pro::SLAC1::mVENUS, $n = 3$; and SLAC1pro::R432A::mVENUS, $n = 3$). Normalized data are shown *Right*. Data were normalized relative to the average stomatal conductance during 30 min of 360-ppm CO_2 exposure before CO_2 elevation. Error bars denote mean ± SEM.

Discussion

The CO_2/HCO_3^- sensors that mediate CO_2 control of stomatal movements remain enigmatic. Both guard cells and mesophyll cells contribute to the stomatal CO_2 response (42, 43). However, the CO_2 sensors that mediate CO_2 control of stomatal movements remain to be determined in either cell type. Previous studies have suggested that intracellular bicarbonate acts as a second messenger in guard cells in mediating CO_2 signal transduction (14, 22, 29). The CO_2 or bicarbonate sensing mechanisms in guard cells remain unknown. In this study, we investigate the mechanisms mediating CO_2/HCO_3^- signaling for CO_2 control of stomatal movements. GaMD simulations predict several candidate bicarbonate interaction sites in SLAC1 (Fig. 1). We have found that residue R256 of SLAC1 is important for CO_2 control of stomatal movements. Mutation of the R256 residue in SLAC1 abrogated the HCO_3^- up-regulation of SLAC1 currents in *Xenopus* oocytes (Fig. 2) and impaired CO_2-induced stomatal closing (Fig. 4) and S-type anion channel activation by HCO_3^- in guard cells (Fig. 7). In contrast, ABA-mediated stomatal closing and ABA activation of S-type anion channels remained intact in SLAC1-R256A–expressing plants (Figs. 6 and 8).

Similar to SLAC1-R256A, mutation of another residue, R321, in SLAC1 also impaired the enhancement of SLAC1 currents by HCO_3^- in *Xenopus* oocytes (Fig. 3). However, in contrast to SLAC1-R256A, expression of the SLAC1-R321A isoform did not affect the rate of CO_2 control of stomatal movements in planta (Fig. 5*A*), suggesting that in its biological protein environment, the R321 site does not affect the physiological CO_2 response. The difference between SLAC1-R256A and SLAC1-R321A isoforms expressed in planta emphasizes that, although helpful, the protein environment in oocytes is simplified and does not necessarily represent the physiological situation in the complex plant system. Further efforts and structural analyses of SLAC1 will be needed to investigate the different behaviors of R256 and R321 in response to CO_2.

The location of the SLAC1-R256 residue at the cytosolic-facing side (Fig. 1*D*) is consistent with the previous finding that bicarbonate ions regulate SLAC1 activity from the intracellular membrane side, not from the extracellular space (29). The location of the R256 residue in the loop between SLAC1 transmembrane domains 2 and 3 (Fig. 1*D*) is consistent with data suggesting that the 10-transmembrane spanning region of SLAC1 functions in the CO_2 response in guard cells (28). The combined computational modeling of bicarbonate-interaction sites within SLAC1 and experimental investigations point to a model in which HCO_3^- ions interact with the SLAC1 protein in dependence of the R256 residue to enhance SLAC1-mediated channel activity in the plasma membrane, thus contributing to CO_2 signal transduction during regulation of stomatal movements.

Gas-exchange and patch clamp analyses on transgenic plants expressing SLAC1-R256A showed that CO_2-regulated stomatal movements and HCO_3^--activated S-type anion channel currents in the guard cell plasma membrane were partially impaired (Figs. 4 and 7). Furthermore, low CO_2 caused a largely intact stomatal

opening response in plants expressing the SLAC1-R432A isoform (Fig. 5*C*). These data suggest that in addition to the HCO_3^- regulation of SLAC1 activity studied here, other CO_2 signal transduction mechanisms exist in guard cells. It has been widely demonstrated that several protein kinases that function upstream of SLAC1 are involved in CO_2 signal transduction in guard cells, leading to the model that CO_2/HCO_3^- may regulate these protein kinase activities in guard cells (14, 15, 19, 21, 23, 24). The primary CO_2/HCO_3^- sensors that regulate these protein kinases remain unknown. A MATE-type transporter, RHC1, was reported to function as a candidate bicarbonate sensor in this response (22). Based on previous and the present findings, we propose the following model for CO_2 signal transduction in guard cells: (*i*) More than one CO_2 signaling branch and CO_2/HCO_3^- sensor is likely to function in CO_2 regulation of stomatal movements; (*ii*) CO_2/HCO_3^- is perceived by a proposed primary CO_2/HCO_3^- sensor and transduced via protein kinases to activate SLAC1 anion channels and other transporters and channels by phosphorylation; and (*iii*) intracellular bicarbonate ions directly up-regulate SLAC1 activity with a requirement for the R256 residue of SLAC1 in this pathway. Taken together, our findings provide evidence that the bicarbonate regulation of SLAC1 anion channels plays an important role in CO_2 control of stomatal movements in planta and that SLAC1 functions not only in anion transport but also as a physiologically relevant secondary HCO_3^- sensor in guard cells.

ABA-induced stomatal closing in the transgenic lines expressing SLAC1-R256A is not distinguishable from the WT SLAC1-expressing lines (Fig. 6). These data suggest that the interaction between HCO_3^- and the SLAC1 protein is physiologically relevant for CO_2, but not for ABA, control of stomatal movements. This hypothesis is supported by a recent study showing that the 10-transmembrane domain region of SLAC1 is required for CO_2-induced stomatal closing via an ABA-independent pathway (28). However, we cannot exclude the possibility that CO_2 also regulates ABA signal transduction in guard cells. To dissect the relationship between ABA and CO_2 signaling pathways in guard cells, further investigations need to be conducted.

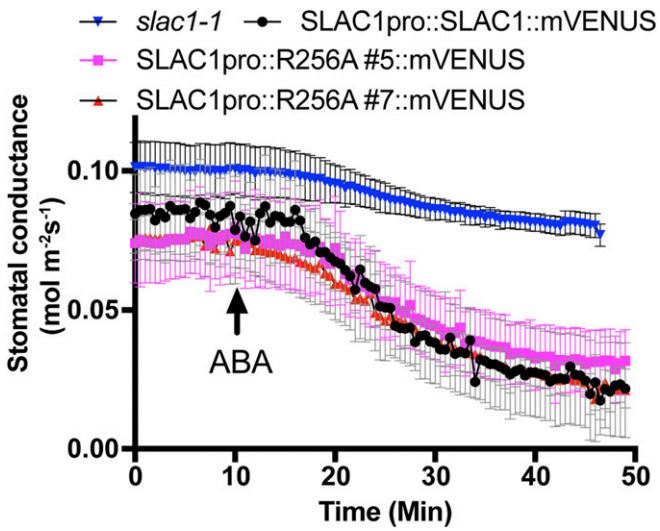

Fig. 6. Point mutation SLAC1-R256A has no effect on ABA-induced stomatal closing in *slac1* transgenic lines. Stomatal conductance of detached leaves from 6-wk-old SLAC1pro::SLAC1::mVENUS (n = 3), SLAC1pro::R256A#5::mVENUS (n = 4), SLAC1pro::R256A#7::mVENUS (n = 4), and *slac1-1*(n = 4) plants in response to 2 μM ABA added to the transpiration stream. Error bars denote mean ± SEM.

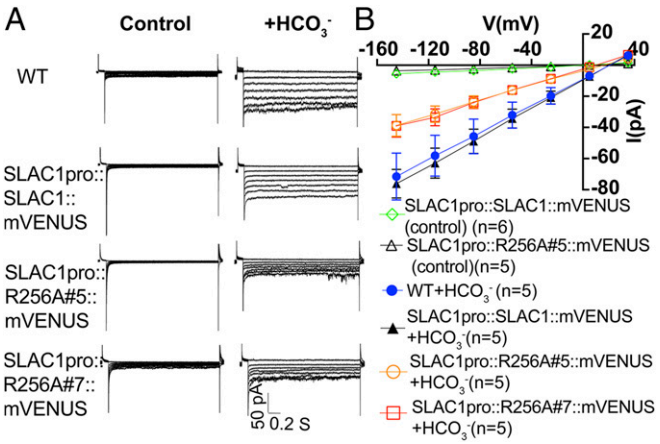

Fig. 7. Effect of point mutation SLAC1-R256A on HCO_3^- activation of S-type anion channel currents in guard cells of *slac1*-transformed lines. (*A*) Representative current recordings in whole-cell patch clamp configuration with guard cell protoplasts from 4- to 6-wk-old WT and transformed slac1 lines. (*B*) Current-voltage relationships of WT and the indicated transformed *slac1* lines in the absence (control) or presence of added HCO_3^- in the cytosol. WT control guard cells and SLAC1-R256A#7 control cells without addition of HCO_3^- showed only small background currents that overlap with the illustrated controls and are not included as data points in *B* for clarity. Error bars show SEM. Note that Figs. 7 and 8 share the same control current–voltage curves, as they were completed within the same datasets.

Some plant membrane transporters, including the nitrate transporter CHL1 (NRT1.1) and the iron uptake transporter IRT1, have been shown to function in both transporting and sensing ionic substrates (44–47). The present study provides evidence that SLAC1 functions as one of the bicarbonate sensors in guard cells in mediating CO_2 control of stomatal movements. However, the precise mechanisms by which intracellular bicarbonate directly affects the activity of SLAC1 remain to be determined. To address this question, the atomic resolution

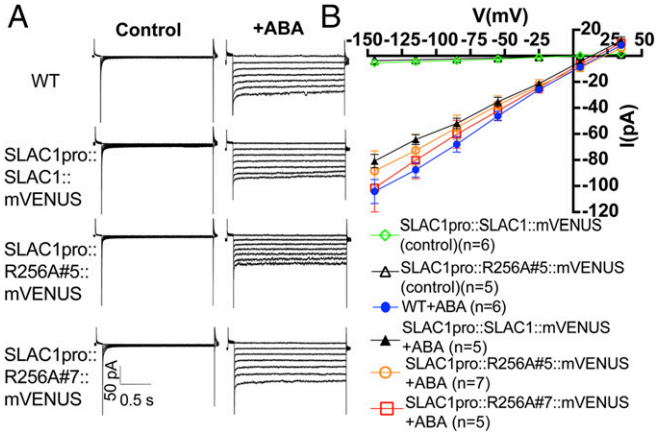

Fig. 8. Mutation of R256A in SLAC1 has no effect on ABA activation of S-type anion channel currents in guard cells of *slac1*-transformed lines. (*A*) Representative current recordings in whole-cell configuration with guard cell protoplasts from 4 to 6 wk-old WT and transformed slac1 lines. (*B*) Current–voltage relationships of WT and the indicated slac1 lines in the absence (control) or presence of 50 μM ABA (+ABA). Note that WT control guard cells and SLAC1-R256A#7 control cells without addition of ABA showed only small background currents that overlap with the illustrated controls and are not included as data points in *B* for clarity. Error bars show SEM. Note that Figs. 7 and 8 share the same control current–voltage curves, as they were completed within the same datasets.

structure of SLAC1 in the presence and absence of HCO_3^- will be needed.

CO_2 control of stomatal movements and gas exchange is of central importance for plant–water relations and leaf temperatures and is predicted to affect larger-scale plant–atmospheric interactions (1). In summary, the findings in this study suggest not only that the SLAC1 anion channel functions in transporting anions for stomatal movements but also that SLAC1 contributes to sense the CO_2/ HCO_3^- signal in the regulation of stomatal movements. Results from this study provide important insight into how plants respond to the diurnal CO_2 concentration changes in leaves (6) and the continuing atmospheric rise in $[CO_2]$.

Materials and Methods

Plant Materials and Growth Conditions. Transgenic plants were generated by *Agrobacterium tumefaciens* (GV3101 pMP90)-mediated transformation as previously described (48). All WT (Col-0), *slac1-1*, *slac1-3*, and transgenic plants were grown in a plant growth chamber (Conviron) with 12 h light/12 h dark with 145 $\mu mol \cdot m^{-2} \cdot s^{-1}$ light, 21 °C, and ~70% relative humidity in potting soil. Four- to 6-wk-old plants were used for patch clamp and gas-exchange experiments.

Site-Directed Mutagenesis and Electrophysiological Analyses. Full-length genomic DNA and cDNA of SLAC1 were cloned into the plant expression vector pGreenII and oocyte expression vector pNB1 by USER cloning strategy as previously described (41, 49). The site-directed mutants were generated by using the Quikchange Site-Directed Mutagenesis Kit (Agilent Technologies) with slight modifications as previously described (50). All point mutations were verified by sequencing. For information on two-electrode voltage clamp in *Xenopus* oocytes and patch clamp in guard cell protoplasts, see *SI Appendix, Supplemental Methods*.

SLAC1 Model System and GaMD. A model of the SLAC1 channel structure was generated using the crystal structure of the *Haemophilus influenzae* TehA homolog (35) as template and applying three separate modeling algorithms: ModBase, iTasser, and RaptorX (36–38). The homology model of the transmembrane region of the SLAC1 structure (residues E179 to F504) generated by ModBase was used in the present study. Molecular graphics and analyses were performed with the UCSF Chimera package (https://www.cgl.ucsf.edu/chimera/) (51). The model was first processed using Protein Preparation Wizard in Maestro (52). This structure was then submitted to the online CHARMM-GUI Membrane Builder (www.charmm-gui.org/) for addition of POPC lipids and a 0.15 M KCl solution. GaMD simulations were performed on the final system using the dual-boost scheme (*SI Appendix, Supplemental Methods*).

Stomatal Conductance Analyses. Leaf stomatal conductance of 5- to 7-wk-old WT (Col-0), *slac1* mutant, and SLAC1 isoform-expressing plants was measured using a portable gas-exchange system (LI-6400 or LI-6400XT; LI-COR) with a leaf chamber (LI-6400-02B; LI-COR) with a setting of 150 $\mu mol \cdot m^{-2} \cdot s^{-1}$ LED light source (10% blue light), 58 to 64% relative humidity, 500 $\mu mol \cdot s^{-1}$ airflow, 21 °C leaf temperature, and 360-ppm CO_2 for stabilization. For CO_2 experiments, data recorded started with 30 min at 360 ppm, followed by 800 ppm for 30 min and followed by 100 ppm for the indicated time periods. In all experiments, the genotypes shown in each figure were grown side by side under the same growth conditions and analyzed within the same time period (10 d). Steady-state stomatal conductance can vary at different times of the year; therefore, each experimental dataset compared genotypes within the same set of plants grown in parallel as reported previously (53). Each figure shows data comparing genotype responses collected within the same experimental set as described previously to avoid time-of-year variation (53). Three independent datasets showed similar findings among genotypes.

For ABA treatments, measurements were conducted by using a portable gas-exchange system (LI-6800; LI-COR) with a leaf chamber (LI-6800-01A; LI-COR) with a setting of 150 $\mu mol \cdot m^{-2} \cdot s^{-1}$ LED light source (10% blue light); 70% relative humidity; 9,000-rpm fan speed; and 21 °C leaf temperature. Detached intact leaves were stabilized at 400-ppm CO_2 with petioles submerged in deionized water. After stabilization, data were recorded initially for 10 min and then for another 40 min with 2 μM ABA final concentration added to the solution in which petioles were submerged.

For both CO_2 and ABA treatments, data were recorded every 30 s by Li-COR gas-exchange analyzers. Data in Figs. 4 and 6 using Li-COR 6400XT and Li-COR 6800 analyzers, respectively, were plotted every 30 s. Data in Fig. 5 using a Li-COR 6400 analyzer were filtered by calculating a mean value of six recorded time points and plotted every 3 min.

ACKNOWLEDGMENTS. We thank Dr. Sebastian Schulze for critical reading of the manuscript. This research was funded by a grant from the National Science Foundation (MCB-1616236) (to W.-J.R. and J.I.S.) and was in part supported by NIH Grant GM060396 (to J.I.S.) and in part by NSF Grant IOS-1444435. Work in the J.A.M. laboratory was supported by the NIH (Grants GM31749 and GM103426) and the San Diego Supercomputer Center.

1. Hetherington AM, Woodward FI (2003) The role of stomata in sensing and driving environmental change. *Nature* 424:901–908.
2. Roelfsema MRG, Hedrich R, Geiger D (2012) Anion channels: Master switches of stress responses. *Trends Plant Sci* 17:221–229.
3. Murata Y, Mori IC, Munemasa S (2015) Diverse stomatal signaling and the signal integration mechanism. *Annu Rev Plant Biol* 66:369–392.
4. Gudesblat GE, Torres PS, Vojnov AA (2009) Stomata and pathogens: Warfare at the gates. *Plant Signal Behav* 4:1114–1116.
5. Underwood W, Melotto M, He SY (2007) Role of plant stomata in bacterial invasion. *Cell Microbiol* 9:1621–1629.
6. Hanstein S, de Beer D, Felle HH (2001) Miniaturised carbon dioxide sensor designed for measurements within plant leaves. *Sens Actuators B Chem* 81:107–114.
7. Mott KA (1988) Do stomata respond to CO(2) concentrations other than intercellular? *Plant Physiol* 86:200–203.
8. LaDeau SL, Clark JS (2001) Rising CO_2 levels and the fecundity of forest trees. *Science* 292:95–98.
9. Medlyn BE, et al. (2001) Stomatal conductance of forest species after long-term exposure to elevated CO_2 concentration: A synthesis. *New Phytol* 149:247–264.
10. Schroeder JI, Keller BU (1992) Two types of anion channel currents in guard cells with distinct voltage regulation. *Proc Natl Acad Sci USA* 89:5025–5029.
11. Raschke K, Shabahang M, Wolf R (2003) The slow and the quick anion conductance in whole guard cells: Their voltage-dependent alternation, and the modulation of their activities by abscisic acid and CO_2. *Planta* 217:639–650.
12. Negi J, et al. (2008) CO_2 regulator SLAC1 and its homologues are essential for anion homeostasis in plant cells. *Nature* 452:483–486.
13. Vahisalu T, et al. (2008) SLAC1 is required for plant guard cell S-type anion channel function in stomatal signalling. *Nature* 452:487–491.
14. Xue S, et al. (2011) Central functions of bicarbonate in S-type anion channel activation and OST1 protein kinase in CO_2 signal transduction in guard cell. *EMBO J* 30:1645–1658.
15. Hashimoto M, et al. (2006) Arabidopsis HT1 kinase controls stomatal movements in response to CO_2. *Nat Cell Biol* 8:391–397.
16. Geiger D, et al. (2009) Activity of guard cell anion channel SLAC1 is controlled by drought-stress signaling kinase-phosphatase pair. *Proc Natl Acad Sci USA* 106:21425–21430.
17. Lee SC, Lan W, Buchanan BB, Luan S (2009) A protein kinase-phosphatase pair interacts with an ion channel to regulate ABA signaling in plant guard cells. *Proc Natl Acad Sci USA* 106:21419–21424.
18. Geiger D, et al. (2010) Guard cell anion channel SLAC1 is regulated by CDPK protein kinases with distinct Ca^{2+} affinities. *Proc Natl Acad Sci USA* 107:8023–8028.
19. Hua D, et al. (2012) A plasma membrane receptor kinase, GHR1, mediates abscisic acid- and hydrogen peroxide-regulated stomatal movement in Arabidopsis. *Plant Cell* 24:2546–2561.
20. Brandt B, et al. (2012) Reconstitution of abscisic acid activation of SLAC1 anion channel by CPK6 and OST1 kinases and branched ABI1 PP2C phosphatase action. *Proc Natl Acad Sci USA* 109:10593–10598.
21. Hõrak H, et al. (2016) A dominant mutation in the HT1 kinase uncovers roles of MAP kinases and GHR1 in CO_2-induced stomatal closure. *Plant Cell* 28:2493–2509.
22. Tian W, et al. (2015) A molecular pathway for CO_2 response in Arabidopsis guard cells. *Nat Commun* 6:6057.
23. Jakobson L, et al. (2016) Natural variation in Arabidopsis Cvi-0 accession reveals an important role of MPK12 in guard cell CO_2 signaling. *PLoS Biol* 14:e2000322.
24. Hiyama A, et al. (2017) Blue light and CO_2 signals converge to regulate light-induced stomatal opening. *Nat Commun* 8:1284.
25. Hu H, et al. (2010) Carbonic anhydrases are upstream regulators of CO2-controlled stomatal movements in guard cells. *Nat Cell Biol* 12:87—18.
26. Chen T, et al. (2017) Absence of OsβCA1 causes a CO_2 deficit and affects leaf photosynthesis and the stomatal response to CO_2 in rice. *Plant J* 90:344–357.
27. Kolbe AR, Brutnell TP, Cousins AB, Studer AJ (2018) Carbonic anhydrase mutants in *Zea mays* have altered stomatal responses to environmental signals. *Plant Physiol* 177:980–989.
28. Yamamoto Y, et al. (2016) The transmembrane region of guard cell SLAC1 channels perceives CO2 signals via an ABA-independent pathway in Arabidopsis. *Plant Cell* 28:557–567.
29. Wang C, et al. (2016) Reconstitution of CO_2 regulation of SLAC1 anion channel and function of CO_2-permeable PIP2;1 aquaporin as CARBONIC ANHYDRASE4 interactor. *Plant Cell* 28:568–582.
30. Miao Y, Feher VA, McCammon JA (2015) Gaussian accelerated molecular dynamics: Unconstrained enhanced sampling and free energy calculation. *J Chem Theory Comput* 11:3584–3595.

31. Hamelberg D, Mongan J, McCammon JA (2004) Accelerated molecular dynamics: A promising and efficient simulation method for biomolecules. *J Chem Phys* 120: 11919–11929.
32. Miao Y, McCammon JA (2017) Gaussian accelerated molecular dynamics: Theory, implementation, and applications. *Annu Rep Comput Chem* 13:231–278.
33. Miao Y, et al. (2016) Accelerated structure-based design of chemically diverse allosteric modulators of a muscarinic G protein-coupled receptor. *Proc Natl Acad Sci USA* 113:E5675–E5684.
34. Miao Y, McCammon JA (2016) G-protein coupled receptors: Advances in simulation and drug discovery. *Curr Opin Struct Biol* 41:83–89.
35. Chen YH, et al. (2010) Homologue structure of the SLAC1 anion channel for closing stomata in leaves. *Nature* 467:1074–1080.
36. Pieper U, et al. (2014) ModBase, a database of annotated comparative protein structure models and associated resources. *Nucleic Acids Res* 42:D336–D346.
37. Yang J, et al. (2015) The I-TASSER Suite: Protein structure and function prediction. *Nat Methods* 12:7–8.
38. Källberg M, et al. (2012) Template-based protein structure modeling using the RaptorX web server. *Nat Protoc* 7:1511–1522.
39. Jo S, Kim T, Iyer VG, Im W (2008) CHARMM-GUI: A web-based graphical user interface for CHARMM. *J Comput Chem* 29:1859–1865.
40. Pang YT, Miao Y, Wang Y, McCammon JA (2017) Gaussian accelerated molecular dynamics in NAMD. *J Chem Theory Comput* 13:9–19.
41. Brandt B, et al. (2015) Calcium specificity signaling mechanisms in abscisic acid signal transduction in Arabidopsis guard cells. *eLife* 4:03599.
42. Mott KA (2009) Opinion: Stomatal responses to light and $CO_{(2)}$ depend on the mesophyll. *Plant Cell Environ* 32:1479–1486.
43. Engineer CB, et al. (2016) CO_2 sensing and CO_2 regulation of stomatal conductance: Advances and open questions. *Trends Plant Sci* 21:16–30.
44. Dubeaux G, Neveu J, Zelazny E, Vert G (2018) Metal sensing by the IRT1 transporter-receptor orchestrates its own degradation and plant metal nutrition. *Mol Cell* 69: 953–964.e5.
45. Ho CH, Lin SH, Hu HC, Tsay YF (2009) CHL1 functions as a nitrate sensor in plants. *Cell* 138:1184–1194.
46. Eide D, Broderius M, Fett J, Guerinot ML (1996) A novel iron-regulated metal transporter from plants identified by functional expression in yeast. *Proc Natl Acad Sci USA* 93:5624–5628.
47. Liu KH, Tsay YF (2003) Switching between the two action modes of the dual-affinity nitrate transporter CHL1 by phosphorylation. *EMBO J* 22:1005–1013.
48. Clough SJ, Bent AF (1998) Floral dip: A simplified method for Agrobacterium-mediated transformation of Arabidopsis thaliana. *Plant J* 16:735–743.
49. Nour-Eldin HH, Nørholm MHH, Halkier BA (2006) Screening for plant transporter function by expressing a normalized Arabidopsis full-length cDNA library in Xenopus oocytes. *Plant Methods* 2:17.
50. Zhang J, Baetz U, Krügel U, Martinoia E, De Angeli A (2013) Identification of a probable pore-forming domain in the multimeric vacuolar anion channel AtALMT9. *Plant Physiol* 163:830–843.
51. Pettersen EF, et al. (2004) UCSF Chimera—A visualization system for exploratory research and analysis. *J Comput Chem* 25:1605–1612.
52. Laio A, Gervasio FL (2008) Metadynamics: A method to simulate rare events and reconstruct the free energy in biophysics, chemistry and material science. *Rep Prog Phys* 71:126601.
53. Azoulay-Shemer T, et al. (2016) Starch biosynthesis in guard cells but not in mesophyll cells is involved in CO_2-induced stomatal closing. *Plant Physiol* 171:788–798.